

# INSIGHT INTO SORPTION AND ANTIOXIDANT PROPERTIES OF ANTIBACTERIAL WOUND DRESSINGS COMPOSED OF VISCOSE FABRICS FUNCTIONALIZED WITH CHITOSAN AND CHITOSAN-BASED NANOPARTICLES

MATEA KORICA,<sup>\*</sup> ZDENKA PERŠIN FRATNIK,<sup>\*\*</sup> LIDIJA FRAS ZEMLJIĆ<sup>✉\*\*</sup> and MIRJANA M. KOSTIĆ<sup>\*\*\*</sup>

<sup>\*</sup>*University of Belgrade, Innovation Center of Faculty of Technology and Metallurgy, 11000 Belgrade, Serbia*

<sup>\*\*</sup>*University of Maribor, Institute of Engineering Materials and Design, Faculty of Mechanical Engineering, 2000 Maribor, Slovenia*

<sup>\*\*\*</sup>*University of Belgrade, Faculty of Technology and Metallurgy, 11000 Belgrade, Serbia*

✉ *Corresponding author: M. Korica, mkorica@tmf.bg.ac.rs*

*Received October 5, 2022*

Wound dressings designed with simultaneously adequate antibacterial, sorption, and antioxidant properties enable proper wound healing. Since the antibacterial properties have already been proven in our previous studies, the sorption and antioxidant properties of raw and differently pretreated (TEMPO-oxidized and TEMPO-oxidized cellulose nanofibrils (TOCN) coated) viscose fabrics (CVs), functionalized with chitosan (CH) and chitosan-based nanoparticles with (NCH+Zn) and without incorporated zinc (NCH), were investigated. The sorption properties were evaluated by absorbency rate and capacity, contact angle, zeta potential, and moisture sorption, whereas the antioxidant properties were determined by the ABTS method. The morphological properties of CVs were investigated by SEM. By using pretreatments, the sorption and antioxidant properties of CVs were improved, while subsequent functionalization with CH, NCH and NCH+Zn decreased both properties. However, TOCN-coated CV functionalized with CH and TEMPO-oxidized CV functionalized with NCH still have sorption and antioxidant properties better than raw CV. The obtained results allow the design of antibacterial wound dressings with predefined sorption and antioxidant properties.

**Keywords:** viscose, TEMPO-oxidation, coating with TEMPO-oxidized cellulose nanofibrils, chitosan, antibacterial wound dressings, predefined sorption and antioxidant properties

## INTRODUCTION

Wound treatment has vital social significance at a scale that extends from the individual to the medical level. Wound dressings play a key role in wound treatment and are widely used for all types of wounds, from minor to life-threatening.<sup>1</sup> Viscose is traditionally used for the production of wound dressings, owing to its nontoxicity, biocompatibility, and bioresorbability.<sup>2</sup> Research and market-oriented modern wound dressings target advanced properties, the most important being antibacterial, sorptive and antioxidant ones.<sup>3</sup> Antibacterial wound dressings are especially desired since they inhibit bacteria at the surface of the wound and thus prevent infections that could delay the healing process.<sup>4</sup> Wound

dressings with the ability to remove excess exudates from the wound bed and consequently reduce the content of nutrients that increase the risk of bacterial growth are also of benefit.<sup>1</sup> Actually, each wound produces an amount of wound secretion.<sup>5</sup> Moreover, the dressing should also provide an adequate moist environment, preventing the wound from being dried out, as this could cause a delay in healing and/or pain during the removal of the bandage. The antioxidant activity of wound dressings also plays a vital role in healing, due to reduction of oxidative processes caused by free radicals. Namely, wounds' oxidative processes caused by free radicals provoke disruption of cellular

functions and various pathological conditions, in which free radicals can overwhelm the antioxidant defenses of the organism.<sup>6</sup>

In manufacturing wound dressings, natural compounds are more than desired, due to their similarity to the extracellular matrix and good acceptance by biological systems, which prevent the immunological reactions often detected towards synthetic compounds.<sup>7,8</sup> Chitosan is a natural amino polysaccharide that is characterized by good antibacterial,<sup>9</sup> antioxidant,<sup>10</sup> sorption,<sup>11</sup> antifungal,<sup>12</sup> antiviral,<sup>13</sup> anti-inflammatory,<sup>14</sup> analgesic,<sup>15</sup> anticancer,<sup>16</sup> hemostatic,<sup>17</sup> anticoagulant,<sup>18</sup> hypocholesterolemic<sup>19</sup> and antidiabetic properties.<sup>20,21</sup> By virtue of its intensive hydrophilicity, chitosan can form a gel at the surface of wound dressings, which could protect the wound.<sup>22</sup> In such a way, chitosan can ensure a convenient environment for angiogenesis, by activating fibroblasts and depositing collagen to accelerate the wound healing process, as proved in preclinical and clinical trials.<sup>23</sup> The latest research using chitosan nanoparticles reported better immune-enhancing,<sup>24</sup> antimicrobial,<sup>25</sup> antimutagenic,<sup>26</sup> and anticancer properties<sup>27</sup> considering bulk chitosan. Nevertheless, to the best of our knowledge, using chitosan nanoparticles and bulk chitosan for improving antioxidant properties has not been compared. Besides chitosan, zinc is also known for its antioxidant properties and is thus used for promoting the wound healing process.<sup>28</sup> Recently, many efforts have been dedicated to incorporating zinc into chitosan nanoparticles to improve the bioactive properties of chitosan and zinc.<sup>29-31</sup> Thus, although there have been conducted studies to investigate the antimicrobial properties of viscose fabrics functionalized with chitosan,<sup>7,8,32-35</sup> no extensive work on viscose functionalized with chitosan, chitosan nanoparticles and chitosan nanoparticles with incorporated zinc has been reported so far.

Since each wound is different, wound dressings with designed desirable properties could enable proper wound healing.<sup>5</sup> In this regard, defining the parameters that influence antibacterial, sorption, and antioxidant properties, when designing wound dressings for targeted use in the therapy of various types of wounds, or wounds in specified stages of healing, would be essential in wound healing treatment.<sup>32</sup> In our previous studies,<sup>7,8</sup> viscose fabrics with antibacterial properties were obtained by functionalization of raw viscose fabrics with

chitosan (CH) and chitosan-based nanoparticles, without and with incorporated zinc (NCH and NCH+Zn), respectively. We continue our research following the pretreatment using two different approaches, *i.e.*, 2,2,6,6-tetramethylpiperidine-1-oxy radical (TEMPO) oxidation and coating with TEMPO-oxidized cellulose nanofibrils (TOCN) before their functionalization with CH, NCH, and NCH+Zn. By TEMPO oxidation and coating with TOCN, carboxyl and aldehyde groups were introduced into the structure of viscose fabrics, which enable improved binding of CH, NCH, and NCH+Zn on viscose fabrics and, consequently, impart antibacterial properties.<sup>7,8,36,37</sup> In this way, the sorption and antioxidant properties of raw and pretreated viscose fabrics, before and after functionalization with CH, NCH and NCH+Zn, were investigated and compared additionally in this study. The sorption properties were determined by measurements of absorbency rate, absorbent capacity, contact angle, zeta potential, and moisture sorption, whereas the antioxidant properties were determined spectrophotometrically using the 2,2'-azinobis(3-ethylbenzothiazoline-6-sulfonic acid) diammonium salt (ABTS) method. To better understand the sorption properties, the morphological properties were also analyzed by scanning electron microscopy (SEM).

## EXPERIMENTAL

### Materials

100% viscose fabric ("15A23 sandy-white viscose", provided by IGR Agence, Celje, Slovenia, <https://igragence.com>), with a weight of 82 g·m<sup>-2</sup>, and fabric count of 400 warp threads/10 cm and 350 weft threads/10 cm, was used as experimental material. Chitosan (CH) (50,000-190,000 Da, 75%–85% deacetylated, Sigma-Aldrich, 448869), hydrochloric acid (HCl), sodium bromide (NaBr), 2,2,6,6-tetramethylpiperidine-1-oxy radical (TEMPO), potassium chloride (KCl), sodium tripolyphosphate (TPP), zinc acetate dihydrate (ZnAc•2H<sub>2</sub>O), *n*-heptane (C<sub>7</sub>H<sub>16</sub>), sodium hydroxide (NaOH), sodium chlorite (NaClO<sub>2</sub>), 13% sodium hypochlorite (NaClO), 2,2'-azinobis(3-ethylbenzothiazoline-6-sulfonic acid) diammonium salt (ABTS) and potassium persulfate (K<sub>2</sub>S<sub>2</sub>O<sub>8</sub>) were purchased from Sigma-Aldrich (Vienna, Austria). All chemicals were of analytical grade and used without purification prior to use. Milli-Q ultrapure water was obtained from a Millipore Direct 8 purification system (Labena, Slovenia).

### Preparation of samples

#### *Preparation of solution for TEMPO-oxidation of viscose fabric*

The solution for TEMPO-oxidation of the viscose fabric was prepared by dissolving TEMPO in 0.05 M sodium phosphate buffer, with pH 7, and subsequent addition of sodium chlorite and sodium hypochlorite. A detailed description of the method has been provided previously.<sup>7</sup>

#### *Preparation of TOCN dispersion for coating of viscose fabric*

TOCN dispersion for coating of viscose fabric was prepared in a two-step process. In the first step, the cotton fibers were TEMPO-oxidized in the TEMPO/sodium bromide/sodium hypochlorite system under alkaline conditions. In the second step, a suspension of TEMPO-oxidized cotton fibers (0.5% solid consistency) in distilled water was then passed through a double cylinder homogenizer (T 25 digital Ultra-Turrax, IKA, Germany) and further sonicated using an ultrasonic homogenizer (WCX 750, Sonics, USA). The obtained TOCN dispersion was centrifuged to remove a small amount of non-fibrillated fraction (<5%). The method has been described in detail previously.<sup>22</sup> The basic parameters of the prepared TOCN dispersion are shown in Table 1.

#### *Pretreatments of viscose fabric*

The viscose fabric was pretreated by two different methods:

1) *TEMPO-oxidation* in the TEMPO/sodium chlorite/sodium hypochlorite system under neutral conditions, for 5 min, at 60 °C. The TEMPO-oxidation was stopped by the addition of ethanol. After that, the TEMPO-oxidized viscose fabric was washed with distilled water, then with ethanol, and dried at room temperature.

2) *Coating with TOCN* in a TOCN dispersion bath, with a ratio of 1:50 and a wet pick-up of 100%, for 30 min, at room temperature. The excess TOCN

dispersion from the TOCN-coated viscose fabric was removed using a laboratory padder (Rapid, Istanbul, Turkey) under a pressure of 2 bars. At the end, TOCN-coated viscose fabric was dried for 30 min at 40 °C in a laboratory oven (Instrumentaria, Zagreb, Croatia).

For a detailed description of the applied methods see previous literature.<sup>7,8</sup> Pretreated fabrics were then conditioned (T = 20±2 °C; RH = 65±4%) prior to further functionalization or characterization.

#### *Preparation of chitosan (CH) solution*

A 0.5% w/v CH solution was prepared by dissolution of CH in distilled water, stirred over night at pH 2.5 adjusted by the addition of 1 M HCl.

#### *Preparation of chitosan-based dispersions without (NCH) and with incorporated zinc (NCH+Zn)*

The NCH dispersion was prepared by an ionotropic gelation process, *i.e.* by dropping TPP solution (1 mg/mL) into the freshly prepared CH solution (in a ratio of 1:1 (w/w)) during 1 h, under constant solution stirring at room temperature. NCH+Zn dispersion was prepared by dropwise addition of 3% solution of ZnAc into freshly prepared NCH dispersion (in a ratio of 10:1 (w/w)). The final pH of NCH and NCH+Zn dispersions was adjusted to pH 5.5 by the addition of 0.5 M NaOH. The basic parameters of the prepared NCH and NCH+Zn dispersions are shown in Table 2.

#### *Functionalization of viscose fabric with chitosan and chitosan-based nanoparticles*

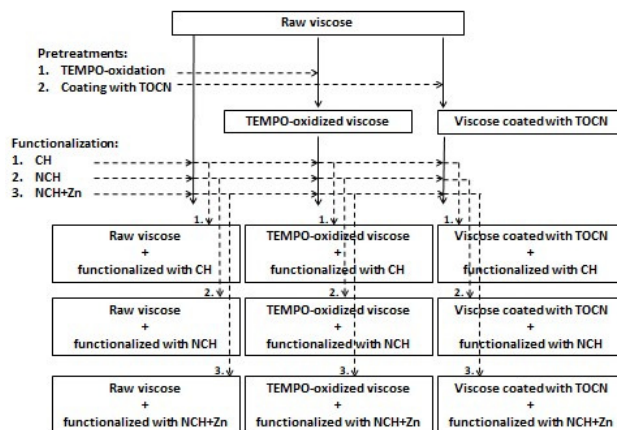
The raw and pretreated viscose fabrics were submerged into the CH solution, NCH dispersion, or NCH+Zn dispersion, at room temperature, for 30 min, and with fabric-liquid bath ratio of 1:50. The fabrics were then squeezed using a laboratory padder (Rapid, Istanbul, Turkey) at a pressure of 2 bars to remove excess liquid, and then dried in a laboratory oven (Instrumentaria, Zagreb, Croatia) at 40 °C, for 30 min. Functionalized fabrics were then conditioned (T = 20±2 °C; RH = 65±4%) prior to characterization.

Table 1  
Solid consistency of TOCN dispersion, zeta potential and hydrodynamic diameter of TOCN in dispersion<sup>32</sup> at pH 8

Sample	Solid consistency (%)	Zeta potential (mV)	Hydrodynamic diameter (nm)
TOCN dispersion	0.500	-39	221

Table 2  
Solid consistency of NCH and NCH+Zn dispersions, zeta potential, and hydrodynamic diameter of NCH and NCH+Zn in dispersions<sup>8,32,38</sup> at pH 5.5

Sample	Solid consistency (%)	Zeta potential (mV)	Hydrodynamic diameter (nm)
NCH dispersion	0.250	32	615
NCH+Zn dispersion	0.225	33	753



Scheme 1: A schematic representation of the preparation of fabric samples

Table 3  
Description and notations of the prepared samples

Description of sample	Notation of sample
TEMPO-oxidized cellulose nanofibrils dispersion	TOCN dispersion
Chitosan solution	CH solution
Chitosan nanoparticles without incorporated zinc dispersion	NCH dispersion
Chitosan nanoparticles with incorporated zinc dispersion	NCH+Zn dispersion
Raw viscose	VIS
TEMPO-oxidized viscose	TEMPO VIS
Viscose coated with TOCN	TOCN VIS
VIS functionalized with CH	VIS/CH
TEMPO VIS functionalized with CH	TEMPO VIS/CH
TOCN VIS functionalized with CH	TOCN VIS/CH
VIS functionalized with NCH	VIS/NCH
TEMPO VIS functionalized with NCH	TEMPO CV/NCH
TOCN VIS functionalized with NCH	TOCN VIS/NCH
VIS functionalized with NCH+Zn	VIS/NCH+Zn
TEMPO VIS functionalized with NCH+Zn	TEMPO VIS/NCH+Zn
TOCN VIS functionalized with NCH+Zn	TOCN VIS/NCH+Zn

Table 4  
Fabric weight, thickness and porosity, as well as percentage of deposited coatings (CH, NCH or NCH+Zn) on the fabric samples

Sample	Fabric weight (g/m <sup>2</sup> )	Thickness (mm)	Porosity (%)	Deposited CH/NCH/NCH+Zn (%)
VIS	82.4 <sup>* **</sup>	0.17 <sup>*</sup>	67.9	
TEMPO VIS	98.6	0.22	70.3	
TOCN VIS	94.5	0.21	70.2	
VIS/CH	96.2	0.23	72.3	0.77 <sup>* **</sup>
TEMPO VIS/CH	93.1	0.25	70.6	1.78 <sup>* **</sup>
TOCN VIS/CH	93.9	0.24	70.4	1.13 <sup>* **</sup>
VIS/NCH	104.6	0.21	72.3	0.43 <sup>* ***</sup>
TEMPO VIS/NCH	100.2	0.23	71.2	1.18 <sup>* ***</sup>
TOCN VIS/NCH	100.7	0.21	71.0	0.63 <sup>* ***</sup>
VIS/NCH+Zn	102.0	0.21	71.8	2.49
TEMPO VIS/NCH+Zn	100.2	0.23	68.4	4.4
TOCN VIS/NCH+Zn	100.8	0.21	68.2	3.05

Previously reported in (\*)<sup>32</sup>, (\*\*) <sup>7</sup> and (\*\*\*)<sup>8</sup>

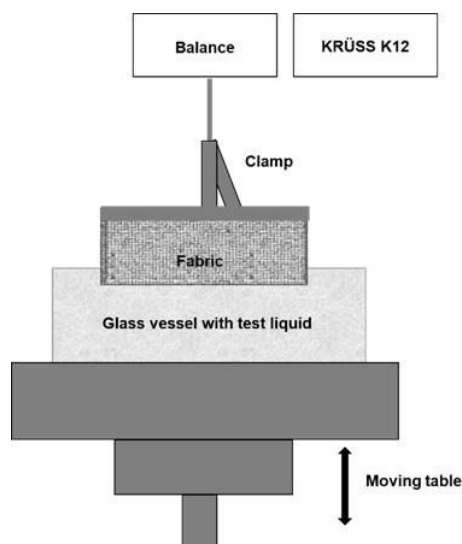


Figure 1: Schematic setup of the capillary rise method used on a KrüssTensiometer K12

The preparation process of the fabric samples is schematically represented in Scheme 1, while the descriptions and notations of the prepared samples are provided in Table 3. The basic parameters of the prepared fabric samples are shown in Table 4.

#### Characterisation methods

##### *Absorbency rate, absorbent capacity and contact angle determination*

The capillary rise method, based on the modified Washburn approach<sup>39</sup> and the Tensiometer Krüss K12 apparatus, was used for determining the absorption capacity, absorbency rate and contact angle of raw and pretreated viscose fabrics, before and after functionalization with CH, NCH and NCH+Zn. In Figure 1, the schematic presentation of the capillary rise method setup is presented.

The fabric samples were cut into rectangular pieces (2 cm×5 cm) and fixed with a clamp within the Krüss Tensiometer K12 apparatus. The glass vessel, filled with 75 mL of wetting liquid, *i.e.*, *n*-heptane and Milli-Q ultrapure water, was put into a glass holder and placed on a moving table. The *n*-heptane was used as a test liquid to determine the constant *c*. Once the constant *c* was known, systematic measurements of sorption properties using Milli-Q ultrapure water were performed. Upon starting the experiment, the moving table was raised until the tested liquid touched the lower edge of the sample. At the moment of the contact, the liquid rose through the sample, as a result of capillary action. The increase in mass of the sample with respect to time was monitored. A more detailed explanation can be found elsewhere.<sup>40</sup> The experimental procedure was repeated at least 10 times for each set of samples in order to obtain statistically significant results.

##### *Moisture sorption determination*

Moisture sorption of the fabrics, prior to and after pretreatment and functionalization, was determined by the gravimetric method, using a Sartorius Infrared moisture analyzer MA35 (Sartorius, Goettingen, Germany), in the operating mode, which involves drying the samples at 105 °C to constant weight.

Moisture sorption was calculated according to Equation 1 as:

$$\text{Moisture sorption} = \frac{m_1 - m_2}{m_2} \times 100 (\%) \quad (1)$$

where  $m_1$  is the mass of fabric before drying (g), and  $m_2$  is the mass of fabric after drying to constant mass (g). For each sample, moisture sorption was determined in triplicate.

##### *Zeta potential measurement*

The zeta potential of differently pretreated and then functionalized viscose fabrics was determined by the streaming potential method, using a SurPASS electrokinetic analyzer (Anton Paar GmbH, Graz, Austria). For a detailed description of the method see previous literature.<sup>7</sup>

##### *Morphology investigation*

The morphology investigation was carried out using a JEOL JSM-5300 scanning electron microscope (JEOL, Tokyo, Japan). Before measurement, the fabric samples were sputtered with gold using a JEOL Ion-Sputter, Model JFC-1100E (JEOL, Tokyo, Japan).

##### *Antioxidant activity determination by ABTS method*

The antioxidant activity of differently pretreated and functionalized viscose fabrics, CH solution, NCH and NCH+Zn dispersion was determined by the ABTS method. 2,2'-azinobis(3-ethylbenzothiazoline-6-sulfonic acid) diammonium salt (ABTS) and potassium persulfate were dissolved in distilled water, in a

concentration of 7 mM and 2.45 mM, respectively. After that, 7 mM ABTS and 2.45 mM potassium persulfate were mixed and stored in the dark, at room temperature, for 12 h in order to produce ABTS radical (ABTS<sup>•+</sup>). Then, 3.9 mL of diluted ABTS<sup>•+</sup> solution was added to the sample (100 mg of viscose fabric or 20 mL of 0.25% CH solution/0.25% NCH dispersion/0.25% NCH+Zn dispersion). The reduction of the ABTS<sup>•+</sup> radical by the sample was evaluated spectrophotometrically, using a UV/VIS spectrophotometer (Cary 60, Agilent, Santa Clara, CA, USA), at a wavelength of 734 nm. The absorbance was measured according to the Beer-Lambert law<sup>41</sup> after 0 min, 15 min, and 60 min. The scavenging capability of ABTS<sup>•+</sup> was calculated according to Equation 2:

$$\text{Inhibition} = \frac{A_{\text{control}} - A_{\text{sample}}}{A_{\text{control}}} \times 100\% \quad (2)$$

where  $A_{\text{control}}$  is the absorbance, measured at the starting concentration of ABTS<sup>•+</sup>, and  $A_{\text{sample}}$  is the absorbance of the remaining concentration of ABTS<sup>•+</sup> in the presence of the sample.

## RESULTS AND DISCUSSION

### Sorption properties

Sorption properties of raw and pretreated viscose fabrics, before and after functionalization with CH, NCH, and NCH+Zn, were characterized in terms of absorbency rate, absorbent capacity, contact angle, zeta potential, and moisture sorption.

Figure 2 presents the absorbency rate and Table 5 presents the absorbency capacity, contact angle, zeta potential and moisture sorption for TEMPO-oxidized and TOCN coated viscose fabrics, before and after functionalization with chitosan-based nanoparticles without and with incorporated zinc.

The absorbency rate is the velocity with which the testing sample is able to absorb the test liquid. According to the slope of the absorbency rate curve, especially in the initial phase of monitoring the sorption process, the velocity could be fast (high slope of the curve) or slow (gentle slope of the curve). As may be noted in Figure 2, the high slope of the absorbency rate curves and high values of mass<sup>2</sup> in the first 25 s for the raw, TEMPO-oxidized and TOCN coated viscose fabrics indicate that these fabrics are able to quickly absorb a large amount of liquid.<sup>32</sup> Thus, in wound dressing applications, such materials would quickly absorb blood and consequently concentrate native elements of coagulation at the site of bleeding, which promotes wound healing.<sup>42</sup>

The absorbent capacity, as determined by the capillary rise method, stands for the amount of liquid uptake in equilibrium. The raw viscose fabric established an equilibrium state after 144 s (Fig. 2) and was able to uptake 0.52 g liquid/g fabric (Table 5). The TEMPO-oxidized viscose fabric attained equilibrium within 25 s (Fig. 2) and was able to absorb 0.65 g of test liquid. The TOCN coated viscose fabric reached the plateau after 190 s (Fig. 2) and was able to uptake the same amount of test liquid as the TEMPO pretreated sample, *i.e.*, 0.64 g liquid/g fabric (Table 5). The functionalization of raw and pretreated viscose fabrics with chitosan and chitosan-based nanoparticles generally decreased their sorption properties, as can be seen from the results presented in Figure 2 and Table 5. More precisely, these fabrics absorbed the test liquid slower and needed longer time to establish the plateau (Fig. 2). The mentioned slower absorbency rate and prolonged time needed for establishing an equilibrium state can be explained by the deposition of chitosan, as well as chitosan-based nanoparticles, on the fiber surfaces (Fig. 3), which blocks cavities and pores on the fiber surfaces, thus hindering the liquid penetration within the fiber.<sup>32</sup> It should be noted that the nanoparticles are dispersed in the residual macromolecule solution of chitosan (they have not been centrifuged), which consequently leads to binding of the nanoparticles onto the surface polymer matrix, leading to the formation of a thin film coating the fiber surface.<sup>43</sup> The surface film, in turn, prevents surface accessibility and availability to the internal fibers' region. In addition, the amine groups of chitosan are less polar than the OH and COOH groups of cellulose, which also leads to a reduction in hydrophilicity and consequently wettability.<sup>44</sup>

The absorbent capacity of the raw and pretreated viscose fabrics generally decreased after functionalization with CH (7.70% for raw, 58.46% for TEMPO-oxidized and 9.38% for TOCN coated viscose fabric), NCH (3.85% for raw, 12.31% for TEMPO-oxidized and 21.88% for TOCN coated viscose fabric), and NCH+Zn (1.93% for raw, 67.69% for TEMPO-oxidized and 64.06% for TOCN coated viscose fabric), as can be noted in Table 5.

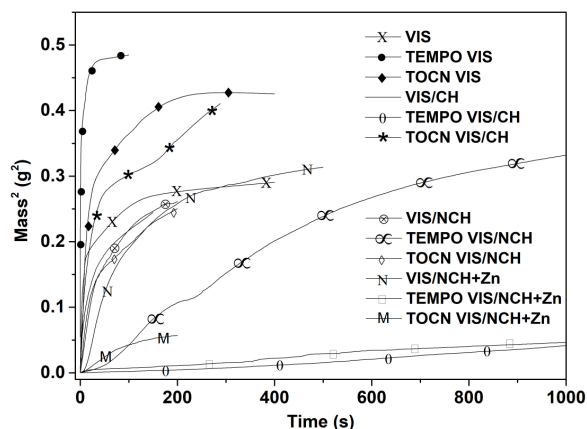


Figure 2: Absorbency rate of raw, TEMPO-oxidized and TOCN coated viscose fabrics before and after functionalization with chitosan and chitosan-based nanoparticles, without and with incorporated zinc

Table 5

Absorbent capacity, contact angle, ratio between maximum negative ( $\zeta_{\max}$ ) and plateau ( $\zeta_{\text{plateau}}$ ) values of zeta potential and moisture sorption of raw, TEMPO-oxidized and TOCN coated viscose fabrics, before and after functionalization with chitosan and chitosan-based nanoparticles, without and with incorporated zinc

Sample	Absorbent capacity (g liquid/g fabric)	Contact angle (°)	$\zeta_{\max}/\zeta_{\text{plateau}}$	Moisture sorption (%)
VIS	0.52±0.04	81±4.72	1.28	8.29±0.23
TEMPO VIS	0.65±0.12	40±9.34	29.21	10.65±0.48
TOCN VIS	0.64±0.05	82±1.11	1.41	9.13±0.55
VIS/CH	0.48±0.08	62±13.23	2.97	8.46±0.16
TEMPO VIS/CH	0.27±0.08	89±0.24	-9.28	10.37±0.50
TOCN VIS/CH	0.58±0.03	29±8.20	0.19	9.61±0.32
VIS/NCH	0.50±0.02	37±9.53	2.35	8.95±0.43
TEMPO VIS/NCH	0.57±0.05	83±1.48	-1.89	10.20±0.17
TOCN VIS/NCH	0.50±0.02	23±9.27	1.54	9.65±0.38
VIS/NCH+Zn	0.51±0.05	61±8.67	0.62	9.15±0.42
TEMPO VIS/NCH+Zn	0.21±0.07	89±0.34	1.15	9.63±0.40
TOCN VIS/NCH+Zn	0.23±0.04	83±2.51	2.58	9.85±0.15

As can be seen from these results, the pretreatments contributed to a greater decrease in the absorbent capacity of functionalized fabrics, probably because of the higher amount of deposited chitosan and chitosan-based nanoparticles (Table 4).<sup>7,8</sup> However, in the case of samples TOCN VIS/CH and TEMPO VIS/NCH, the pretreatments improved their final absorbent capacity: TOCN VIS/CH showed 20.83% higher absorbent capacity, compared to VIS/CH, while TEMPO VIS/NCH showed 14.00% higher absorbent capacity, compared to VIS/NCH.

The contact angle of the raw viscose fabric is 81°, of TEMPO-oxidized – 40° and of TOCN coated – 82° (Table 5). TEMPO-oxidation introduces hydrophilic functional groups, which explains the decrease in the contact angle of viscose fabric. The fact is that the decrease of the

contact angle was further induced by the pronounced surface roughness of TEMPO-oxidized viscose fibers (Fig. 3), since it was found that the contact angle decreases with increasing roughness of the fibers.<sup>45</sup> Surprisingly, a slight increase in the contact angle was noticed after coating with TOCN, but the increase was not statistically significant (according to the t-test), thus one could see unchanged hydrophilicity after coating with TOCN. Considering the fact that coating of viscose fabric with TOCN leads to the introduction of hydrophilic functional groups on its surface,<sup>7,8</sup> the statistically insignificant change in its contact angle after the coating can be explained by strong interactions between the hydrophilic functional groups of TOCN preventing their participation in interactions with water molecules.

The contact angles of the raw and TOCN coated viscose fabrics after functionalization with chitosan and chitosan-based nanoparticles decreased, while the contact angle of TEMPO-oxidized viscose fabric after functionalization with chitosan and chitosan-based nanoparticles increased (Table 5). It is known that chitosan is an extremely hydrophilic molecule,<sup>22</sup> so a decrease of contact angles, *i.e.*, increase in hydrophilicity of raw and TOCN coated viscose fabrics surfaces after chitosan and chitosan-based nanoparticles deposition was expected. However, in the case of

TEMPO-oxidized viscose fabric, there was an increase in contact angle, *i.e.*, a decrease in the hydrophilicity of its surface after functionalization, probably due to the established interactions between TEMPO-oxidized viscose fabric and chitosan, as well as chitosan-based nanoparticles, which decreased the amount of their free hydrophilic groups. The deposition of chitosan, as well as chitosan-based nanoparticles, on the TEMPO-oxidized fiber surface (Fig. 3) probably decreased its roughness and thus further contributed to the increase in contact angle.

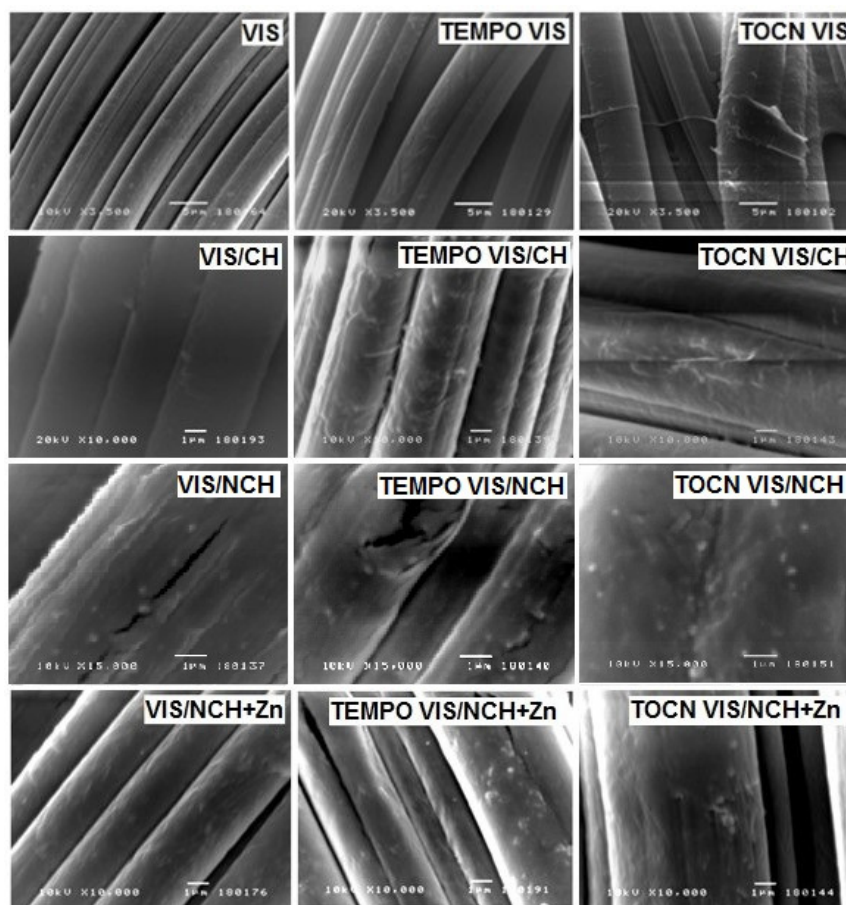


Figure 3: SEM images of raw, TEMPO-oxidized and TOCN coated viscose fabrics before and after functionalization with chitosan and chitosan-based nanoparticles, without and with incorporated zinc

The absorbency capacity of fabrics is related to their swelling degree. The swelling of fabrics during liquid absorption affects the position of the electrokinetic shear plane and thus their zeta potential values. With an increase in the swelling degree, the zeta potential value decreases, while the sign of the zeta potential value does not

change. Also, with an increasing swelling degree of fabrics, the ratio between the maximum negative ( $\zeta_{\max}$ ) and the plateau ( $\zeta_{\text{plateau}}$ ) values of the zeta potential increases.<sup>46</sup> As opposed to the raw and TOCN coated viscoses, the increase of the  $\zeta_{\max}/\zeta_{\text{plateau}}$  value for TEMPO-oxidized viscose (Table 5) demonstrates its enhanced swelling



degree caused by changes in the fibers' inner structure formed during TEMPO-oxidation.<sup>47</sup> The performed zeta potential measurements unequivocally indicate that increased swelling of TEMPO-oxidized viscose contributes to its higher absorbent capacity.<sup>48-50</sup> As expected, for the raw and TOCN coated viscoses, the  $\zeta_{\max}/\zeta_{\text{plateau}}$  values are similar (Table 5), demonstrating that coating with TOCN did not cause significant changes in the inner structure of viscose. Given that, it can be concluded that the higher absorbent capacity of TOCN coated viscose, in comparison with the raw one, is a consequence of the formation of a thin polymer film of TOCN, with high hydrophilicity,<sup>22</sup> on the viscose fibers.

TEMPO-oxidized (10.65%), as well as TOCN coated (9.13%) viscose fabrics, have higher values of moisture sorption than the raw viscose fabric (8.29%) (Table 5). This trend can be explained by the introduction of hydrophilic functional groups in the case of TOCN coated viscose fabrics,<sup>7,8,22</sup> and in the case of TEMPO-oxidized viscose fabrics, additionally by structural changes and higher surface roughness,<sup>7,8,22,48,51,52</sup> which makes the inner parts of the TEMPO-oxidized viscose fibers more accessible to the penetration of gases, liquids, ions, and particles. All these are supported by SEM, as will be discussed below.

Unlike the absorbency rate, absorbent capacity and contact angle, moisture sorption of the raw and pretreated viscose fabrics after functionalization with chitosan and chitosan-based nanoparticles has not changed significantly (Table 5).<sup>32</sup>

While zeta potential measurements provided information on changes in fibers' inner structure, SEM analysis provided additional information on changes in fibers' outer surface. TEMPO-oxidized viscose fibers show signs of damage on their surface, formed during TEMPO-oxidation, in the form of cracks of greater or lesser depth (Fig. 3). It is likely that the noticed damage on the surface of TEMPO-oxidized viscose fibers additionally contributed to facilitated liquid sorption in their inner structure, increased swelling degree, and consequently higher absorbent capacity. In the case of TOCN coated viscose fibers, a thin polymer film of TOCN on the viscose fibers is noticeable (Fig. 3). In this way, the assumption that the higher absorbent capacity of TOCN coated viscose, in comparison with the raw one, is the consequence of the formed thin polymer film of TOCN, with high

hydrophilicity, due to a higher amount of polar groups on the viscose fibers was confirmed.

### Antioxidant properties

Antioxidant molecules/materials 'neutralize' free radicals, whereby the antioxidant molecules/materials themselves become oxidized.<sup>53</sup> In this way, free radicals having one or more unpaired electrons in their structure, allowing them to react easily with other molecules/materials, are prevented from generate new free radicals.

The inhibition of ABTS radicals by the CH solution, and NCH and NCH+Zn dispersion was measured after 0, 15 and 60 min (Fig. 4). For the CH solution, as well as for the NCH and NCH+Zn dispersions, increased inhibition of ABTS radicals during 60 min was observed. The fact is that chitosan has antioxidant properties, due to the 'neutralization' of free radicals with hydrogen from its hydroxyl and amino groups,<sup>54,55</sup> but not as powerful as those of some other natural antioxidant molecules, such as lycopene, coenzyme Q10, alpha-lipoic acid, ellagic acid, and vitamin C.<sup>56</sup> From Figure 4, it can be seen that the CH solution, as well as the NCH and NCH+Zn dispersions achieved low inhibition of ABTS radicals after 60 min: 9% for CH solution, 11% for NCH dispersion, and 2% for NCH+Zn dispersion. The observed slightly increased inhibition of ABTS radicals for the NCH dispersion, compared to the CH solution, was expected, since it is known that chitosan nanoparticles have many enhanced properties compared to bulk chitosan. However, even though the antioxidant effect of zinc is realized in wound healing through the replacement of redox active molecules at critical sites in cell membranes and proteins, as well as the induction of synthesis of metallothionein, sulfhydryl-rich proteins that protect against free radicals,<sup>57</sup> the NCH+Zn dispersion showed decreased inhibition of ABTS radicals, compared to the CH solution and the NCH dispersion. This trend is probably the aftermath of the irreversible binding of zinc with chitosan nanoparticles during the preparation of the NCH+Zn dispersion, considering that chitosan chelates metals.<sup>58</sup>

The inhibition of ABTS radicals by the raw and pretreated viscose fabrics, before and after functionalization with chitosan and chitosan-based nanoparticles, measured after 0, 15 and 60 min can be seen in Figure 5. For all investigated fabrics, increased inhibition of ABTS radicals

during 60 min was observed. Considering its chemical structure, *i.e.*, the presence of hydroxyl, carboxyl and aldehyde groups, cellulose as well as cellulose-based materials, such as viscose, has the potential to ‘neutralize’ free radicals by donation of hydrogen ions. However, the exact mechanism of the antioxidant activity of cellulose and cellulose-based materials is still unknown.<sup>59</sup> Figure 5 shows that the raw and the pretreated viscose fabrics achieve significant inhibition of ABTS radicals after 60 min: 25% for VIS, 48% for TOCN VIS, and 97% for TEMPO VIS. The inhibition of ABTS radicals is correlated with their carboxyl groups content: 0.064 mmol·g<sup>-1</sup> cellulose for VIS, 0.086 mmol·g<sup>-1</sup> cellulose for

TOCN VIS, and 0.438 mmol·g<sup>-1</sup> cellulose for TEMPO VIS,<sup>7,8,32</sup> thus, increased carboxyl group content yields higher inhibition of ABTS radicals. The carboxyl groups of the raw viscose fabric are in COOH form, while that in the pretreated viscose fabrics are in COONa form. Sodium ions from COONa groups of the pretreated viscose fabrics are more susceptible to dissociation than hydrogen ions from OH, COOH, and CHO groups of the raw viscose fabric. In addition to the increased carboxyl group contents, it is likely that more susceptible dissociation of sodium ions than hydrogen ions played an additional role in improving the inhibition of ABTS radicals by the pretreated viscose fabrics.

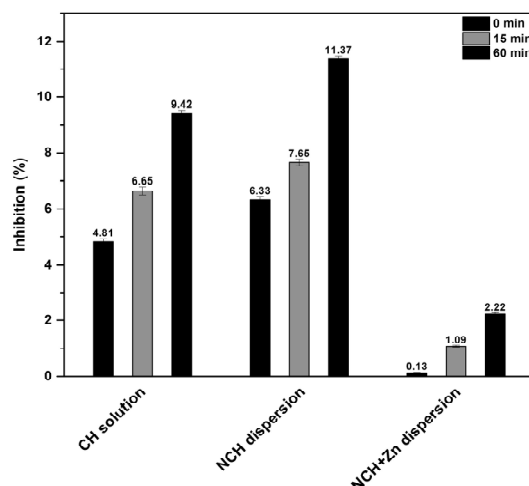


Figure 4: Antioxidant activity of chitosan and chitosan-based nanoparticles without and with incorporated zinc during 60 min

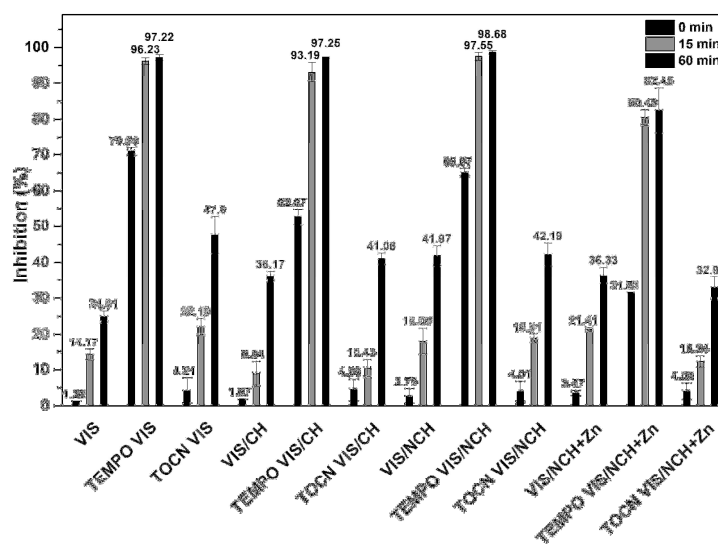


Figure 5: Antioxidant activity of raw, TEMPO-oxidized and TOCN coated viscose fabrics before and after functionalization with chitosan and chitosan-based nanoparticles, without and with incorporated zinc during 60 min

After functionalization with chitosan and chitosan-based nanoparticles, the raw viscose fabric generally achieved higher inhibition of ABTS radicals, while pretreated viscose fabrics generally achieved lower inhibition of ABTS radicals (Fig. 5). Although the CH solution, as well as the NCH and NCH+Zn dispersions, showed lower inhibition of ABTS radicals than the raw viscose fabric, higher inhibition of ABTS radicals by the raw viscose fabric after functionalization with CH solution and NCH and NCH+Zn dispersions was achieved. This trend can be explained, to the greatest extent, by reversible binding of CH, NCH and NCH+Zn onto/into the raw viscose fabric during functionalization, which was noticed in our previous studies,<sup>7,8</sup> and subsequent desorption of CH, NCH, and NCH+Zn. In this way, in addition to the hydrogen donating groups of CH, NCH, and NCH+Zn, the hydrogen donating groups of the raw viscose fabric can also participate in the inhibition of ABTS radicals. Considering that the CH solution and NCH and NCH+Zn dispersions showed lower inhibition of ABTS radicals than the pretreated viscose fabrics, lower inhibition of ABTS radicals by the pretreated viscose fabrics functionalized with CH solution and NCH and NCH+Zn dispersion can be explained, to the greatest extent, by irreversible binding of CH, NCH, and NCH+Zn onto/into the pretreated viscose fabrics during functionalization, which was noticed in our previous studies.<sup>7,8</sup> In other words, the permanent deposition of CH, NCH, and NCH+Zn onto/into pretreated viscose fabrics, based on the physical barrier principle, reduces the initial ability of pretreated viscose fabrics to inhibit ABTS radicals. Also, the mentioned irreversible binding probably leads to the decreased availability of hydrogen donating groups of CH, NCH, and NCH+Zn and thus to an additional decrease in the inhibition of ABTS radicals.

Fras Zemljič *et al.*<sup>33</sup> also investigated the antioxidant properties of raw and pretreated viscose fabrics functionalized with CH and NCH. In contrast to TEMPO-oxidation and coating with TOCN, Fras Zemljič *et al.* performed periodate oxidation, followed by conversion of aldehyde groups to carboxyl groups as pretreatment of viscose fabric. Compared to Fras Zemljič *et al.*,<sup>33</sup> in our study, we obtained raw and pretreated viscose fabrics functionalized with CH and NCH with higher inhibition of ABTS radicals after 60

min. The raw viscose fabrics functionalized with CH and NCH achieved higher inhibition of ABTS radicals after 60 min by 17% and 24%, respectively. The reason for this probably lies in the higher amount of CH and NCH deposited on the viscose fabric, which was made possible by the functionalization conditions designed in our study. The pretreated viscose fabrics functionalized with CH and NCH achieved higher inhibition of ABTS radicals after 60 min by 76%, 83%, 20%, and 27% for TEMPO VIS/CH, TEMPO VIS/NCH, TOCN VIS/CH, and TOCN VIS/NCH, respectively. In the case of the pretreated viscose fabric functionalized with CH and NCH, higher inhibition of ABTS radicals can be explained by two reasons. The first reason is related to the amount and distribution of carboxyl groups in the pretreated viscose fabrics. TEMPO VIS has a higher amount of carboxyl groups than periodate oxidized viscose fabric with its converted aldehyde to carboxyl groups (PER VIS), while TOCN VIS has a lower amount of carboxyl groups than PER VIS. However, both TEMPO VIS and TOCN VIS achieved higher inhibition of ABTS radicals than PER VIS. The higher amount of carboxyl groups in TEMPO VIS led to the higher initial ability of TEMPO VIS to inhibit ABTS radicals (97%) than of PER VIS (22%). Despite the lower amount of carboxyl groups in TOCN VIS, TOCN VIS showed a higher initial ability to inhibit ABTS radicals (47%) than PER VIS (22%). Since the carboxyl groups in TOCN VIS are distributed only on its surface, it is likely that the carboxyl groups distributed on the surface of the fabrics participate to the greatest extent in the inhibition of ABTS radicals during the first 60 min. After functionalization with CH and NCH, there was an inevitable reduction in the initial ability of TEMPO VIS, TOCN VIS, and PER VIS to inhibit ABTS radicals, whereby TEMPO VIS and TOCN VIS remained higher inhibition of ABTS radicals than PER VIS. The second reason is related to the decreased availability of hydrogen donating groups of CH and NCH deposited on TEMPO VIS, TOCN VIS, and PER VIS, which cause additional reduction in the initial ability of TEMPO VIS, TOCN VIS, and PER VIS to inhibit ABTS radicals. That additional reduction in the initial ability of TEMPO VIS, TOCN VIS, and PER VIS to inhibit ABTS radicals, after functionalization with CH and NCH, occurred in

a way that TEMPO VIS and TOCN VIS exhibited higher inhibition of ABTS radicals than PER VIS.

In accordance with the results obtained for inhibition of ABTS radicals by the CH solution, and the NCH and NCH+Zn dispersions, it was noticed that the raw and the pretreated viscose fabrics functionalized with NCH dispersion have higher inhibition of ABTS radicals than their counterparts functionalized with CH solution (Fig. 5). Also, the raw and the pretreated viscose fabrics functionalized with NCH+Zn dispersion have lower inhibition of ABTS radicals than their counterparts functionalized with NCH dispersion. It is important to point out that lower inhibition of ABTS radicals by the raw and the pretreated viscose fabrics functionalized with NCH+Zn dispersion than their counterparts functionalized with NCH dispersion, besides the irreversible binding of zinc with NCH during the preparation of NCH+Zn dispersion, is probably also a consequence of the irreversible binding of zinc with viscose fabrics during their functionalization with NCH+Zn dispersion. In our previous study,<sup>8</sup> the irreversible binding of zinc with viscose fabrics during their functionalization with NCH+Zn dispersion was confirmed. Namely, a certain amount of free zinc ions, present in the NCH+Zn dispersion, were irreversibly bound directly to the viscose fabrics during their functionalization with the NCH+Zn dispersion. In

the case of irreversible binding of zinc to NCH, the releasing of zinc is disabled and at the same time, the amount of available chitosan amino groups responsible for hydrogen donating is decreased. In the case of irreversible binding of zinc to viscose fabrics, the releasing of zinc is also disabled and at the same time the amounts of available viscose hydroxyl, carboxyl and aldehyde groups, responsible for hydrogen/sodium donating, are decreased. To summarize, the irreversible binding of zinc with NCH and viscose fabrics probably led to two effects responsible for the lower inhibition of ABTS radicals: 1) disabled release of zinc and 2) decreased availability of hydrogen/sodium donating groups of chitosan and viscose fabrics. Finally, the synergistic influence of the mentioned effects was consequently reflected in the lower inhibition of ABTS radicals by the raw and the pretreated viscose fabrics functionalized with the NCH+Zn dispersion, compared to their counterparts functionalized with the NCH dispersion. In any case, from Figure 5, it can be seen that the pretreatments improve the antioxidant properties of viscose fabrics functionalized with CH solution and NCH and NCH+Zn dispersion, whereby TEMPO-oxidation represents a more effective pretreatment than coating with TOCN.

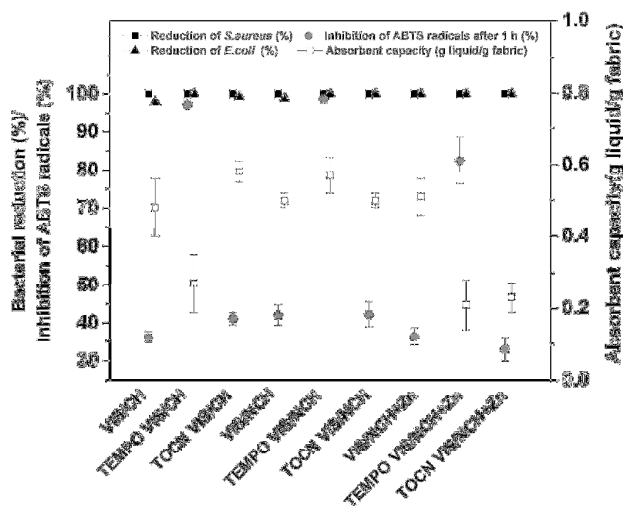


Figure 6: Antibacterial,<sup>7,8,32</sup> sorption and antioxidant properties of raw, TEMPO-oxidized and TOCN coated viscose fabrics after functionalization with chitosan and chitosan-based nanoparticles, without and with incorporated zinc

To summarize, the raw and pretreated and then functionalized viscose fabrics have good antibacterial properties, as proven in our previous study,<sup>7,8</sup> while their sorption and antioxidant

properties vary in a wide range. In Figure 6, the correlations between antibacterial, antioxidant and sorption properties of the raw and pretreated and then functionalized viscose fabrics are presented,

offering the possibility to choose an adequate modification process for viscose fabric for successful application in different types of wounds or wounds in certain stages of healing.

## CONCLUSION

In this study, raw and pretreated (TEMPO-oxidized and TOCN coated) viscose fabrics were functionalized with chitosan (CH) and chitosan-based nanoparticles without (NCH) and with incorporated zinc (NCH+Zn), aiming to obtain materials suitable as wound dressings exhibiting, besides antimicrobial, predefined sorption and antioxidant properties. For this purpose, since the antimicrobial properties were already examined in our previous study, the sorption and antioxidant properties of the mentioned samples were investigated and compared in detail, using tensiometry, zeta potential, scanning electron microscopy, and the ABTS method. Using the pretreatments alone improved both the sorption and antioxidant properties of viscose fabrics, with more pronounced in the case of TEMPO-oxidation. On the other hand, using the pretreatment in combination with functionalization, the sorption properties worsen in the case of the raw and pretreated viscose fabrics (after functionalization with CH, NCH, and NCH+Zn). Improved antioxidant properties of raw viscose fabric were obtained after functionalization with CH, NCH, and NCH+Zn (more pronounced in the case of functionalization with NCH), while using pretreatments prior to functionalization with CH, NCH and NCH+Zn, the antioxidant properties worsened. A significant increase in the sorption and antioxidant properties of viscose fabric after the pretreatments enabled TOCN coated viscose fabric functionalized with CH and TEMPO-oxidized viscose fabric functionalized with NCH to achieve a simultaneous increase in the sorption and antioxidant properties, compared to those of the raw viscose fabric. Besides obtaining viscose fabrics functionalized with CH, NCH and NCH+Zn, with simultaneously increased sorption and antioxidant properties in comparison with raw viscose fabric, a great contribution of this study lies also in the possibility to establish correlations between the parameters of obtaining viscose fabrics functionalized with CH, NCH, and NCH+Zn and their sorption and antioxidant properties. These correlations enable obtaining of viscose fabrics functionalized with CH, NCH, and NCH+Zn, which are suitable for the production of

antibacterial wound dressings with predefined sorption and antioxidant properties, and for targeted use in the treatment of various types of wounds or wounds in certain stages of healing.

**ACKNOWLEDGMENTS:** This work was supported by the Ministry of Education, Science and Technological Development of the Republic of Serbia (Contract No. 451-03-68/2022-14/200135 and Contract No. 451-03-68/2022-14/200287). The financial support from the Slovenian Research Agency (Research Programs P2-0118: Textile chemistry and advanced textile materials) is also gratefully acknowledged.

## REFERENCES

- <sup>1</sup> M. Naseri-Nosar and Z. M. Ziora, *Carbohydr. Polym.*, **189**, 379 (2018), <https://doi.org/10.1016/j.carbpol.2018.02.003>
- <sup>2</sup> W. Zhong, "An Introduction to Healthcare and Medical Textiles", DEStech Publications, Inc., 2013
- <sup>3</sup> A. E. Stoica, C. Chircov and A. M. Grumezescu, *Molecules*, **25**, 2699 (2020), <https://doi.org/10.3390/molecules25112699>
- <sup>4</sup> A. Bal-Öztürk, B. Özkahraman, Z. Özbaş, G. Yaşayan, E. Tamahkar *et al.*, *J. Biomed. Mater. Res.*, **109**, 703 (2021), <https://doi.org/10.1002/jbm.b.34736>
- <sup>5</sup> E. Rezvani Ghomi, S. Khalili, S. Nouri Khorasani, R. Esmaeely Neisiany and S. Ramakrishna, *J. Appl. Polym. Sci.*, **136**, 47738 (2019), <https://doi.org/10.1002/app.47738>
- <sup>6</sup> I. M. Comino-Sanz, M. D. López-Franco, B. Castro and P. L. Pancorbo-Hidalgo, *Trials*, **21**, 1 (2020), <https://doi.org/10.1186/s13063-020-04445-5>
- <sup>7</sup> M. Korica, Z. Peršin, S. Trifunović, K. Mihajlovski, T. Nikolić *et al.*, *Materials*, **12**, 3144 (2019), <https://doi.org/10.3390/ma12193144>
- <sup>8</sup> M. Korica, Z. Peršin, L. Fras Zemljič, K. Mihajlovski, B. Dojčinović *et al.*, *Materials*, **14**, 3762 (2021), <https://doi.org/10.3390/ma14133762>
- <sup>9</sup> J. Li and S. Zhuang, *Eur. Polym. J.*, **138**, 1 09984 (2020), <https://doi.org/10.1016/j.eurpolymj.2020.109984>
- <sup>10</sup> D. G. Ivanova and Z. L. Yaneva, *Biores. Open Access*, **9**, 64 (2020), <https://doi.org/10.1089/biores.2019.0028>
- <sup>11</sup> H. Hamedi, S. Moradi, S. M. Hudson and A. E. Tonelli, *Carbohydr. Polym.*, **199**, 445 (2018), <https://doi.org/10.1016/j.carbpol.2018.06.114>
- <sup>12</sup> A. Verlee, S. Mincke and C. V. Stevens, *Carbohydr. Polym.*, **164**, 268 (2017), <https://doi.org/10.1016/j.carbpol.2017.02.001>
- <sup>13</sup> S. N. Chirkov, *Appl. Biochem. Microbiol.*, **38**, 1 (2002), <https://doi.org/10.1023/A:1013206517442>
- <sup>14</sup> K. Azuma, T. Osaki, S. Minami and Y. Okamoto, *J. Funct. Biomater.*, **6**, 33 (2015), <https://doi.org/10.3390/jfb6010033>

- <sup>15</sup> Y. Okamoto, K. Kawakami, K. Miyatake, M. Morimoto, Y. Shigemasa *et al.*, *Carbohydr. Polym.*, **49**, (2002), [https://doi.org/10.1016/S0144-8617\(01\)00316-2](https://doi.org/10.1016/S0144-8617(01)00316-2)
- <sup>16</sup> H. S. Adhikari and P. N. Yadav, *Int. J. Biomater.*, **2018**, 2952085 (2018), <https://doi.org/10.1155/2018/2952085>
- <sup>17</sup> Z. Hu, D.-Y. Zhang, S.-T. Lu, P.-W. Li and S.-D. Li, *Mar. Drugs*, **16**, 273 (2018), <https://doi.org/10.3390/md16080273>
- <sup>18</sup> S.-H. Chang and J.-J. Huang, *Surf. Coat. Technol.*, **206**, 4959 (2012), <https://doi.org/10.1016/j.surfcoat.2012.05.121>
- <sup>19</sup> Y. Maezaki, K. Tsuji, Y. Nakagawa, Y. Kawai, M. Akimoto *et al.*, *Biosci. Biotech. Biochem.*, **57**, 1439 (1993), <https://doi.org/10.1271/bbb.57.1439>
- <sup>20</sup> F. Karadeniz and S.-K. Kim, *Adv. Food Nutr. Res.*, **73**, 33 (2014), <https://doi.org/10.1016/B978-0-12-800268-1.00003-2>
- <sup>21</sup> D.-H. Ngo and S.-K. Kim, *Adv. Food Nutr. Res.*, **73**, 15 (2014), <https://doi.org/10.1016/B978-0-12-800268-1.00002-0>
- <sup>22</sup> M. Korica, L. Fras Zemljic, M. Bračić, R. Kargl, S. Spirk *et al.*, *Holzforschung*, **73**, 93 (2019), <https://doi.org/10.1515/hf-2018-0094>
- <sup>23</sup> M. E. Aljghami, S. Saboor and S. Amini-Nik, *Ann. Biomed. Eng.*, **47**, 659 (2019), <https://doi.org/10.1007/s10439-018-02186-w>
- <sup>24</sup> Z.-S. Wen, Y.-L. Xu, X.-T. Zou and Z.-R. Xu, *Mar. Drugs*, **9**, 1038 (2011), <https://doi.org/10.3390/md9061038>
- <sup>25</sup> L. Qi, Z. Xu, X. Jiang, C. Hu and X. Zou, *Carbohydr. Res.*, **339**, 2693 (2004), <https://doi.org/10.1016/j.carres.2004.09.007>
- <sup>26</sup> Z. B. Yu, D. R. Chai and H. Tao, *Occup. Health*, **19**, 4 (2007)
- <sup>27</sup> L. Qi, Z. Xu and M. Chen, *Eur. J. Cancer*, **43**, 184 (2007), <https://doi.org/10.1016/j.ejca.2006.08.029>
- <sup>28</sup> P.-H. Lin, M. Sermersheim, H. Li, P. H. U. Lee, S. M. Steinberg *et al.*, *Nutrients*, **10**, 16 (2018), <https://doi.org/10.3390/nu10010016>
- <sup>29</sup> P. Deshpande, A. Dapkekar, M. D. Oak, K. M. Paknikar and J. M. Rajwade, *Carbohydr. Polym.*, **165**, 394 (2017), <https://doi.org/10.1016/j.carbpol.2017.02.061>
- <sup>30</sup> K. Saravanakumar, E. Jeevithan, R. Chelliah, K. Kathiresan, W. Wen-Hui *et al.*, *Int. J. Biol. Macromol.*, **119**, 1144 (2018), <https://doi.org/10.1016/j.ijbiomac.2018.08.017>
- <sup>31</sup> R. C. Choudhary, R. V. Kumaraswamy, S. Kumari, S. S. Sharma, A. Pal *et al.*, *Int. J. Biol. Macromol.*, **127**, 126 (2019), <https://doi.org/10.1016/j.ijbiomac.2018.12.274>
- <sup>32</sup> M. Korica, PhD Dissertation, University of Belgrade, 2020
- <sup>33</sup> L. Fras Zemljic, Z. Peršin, O. Šauperl, A. Rudolf and M. Kostić, *Text. Res. J.*, **88**, 2519 (2018), <https://doi.org/10.1177/0040517517725117>
- <sup>34</sup> L. Fras Zemljic, O. Sauperl, I. But, A. Zabret and M. Lusicky, *Text. Res. J.*, **81**, 1183 (2011), <https://doi.org/10.1177/0040517510397572>
- <sup>35</sup> L. Fras Zemljic, J. Volmajer, T. Ristić, M. Bracic, O. Sauperl *et al.*, *Text. Res. J.*, **84**, 819 (2013), <https://doi.org/10.1177/0040517513512396>
- <sup>36</sup> A. Isogai, T. Hänninen, S. Fujisawa and T. Saito, *Prog. Polym. Sci.*, **86**, 122 (2018), <https://doi.org/10.1016/j.progpolymsci.2018.07.007>
- <sup>37</sup> D. Cheng, Y. Wen, X. An, X. Zhu and Y. Ni, *Carbohydr. Polym.*, **151**, 326 (2016), <https://doi.org/10.1016/j.carbpol.2016.05.083>
- <sup>38</sup> M. D. Korica, A. Kramar, Z. Peršin Fratnik, B. Obradović, M. M. Kuraica *et al.*, *Polymers*, **14**, 4152 (2022), <https://doi.org/10.3390/polym14194152>
- <sup>39</sup> E. W. Washburn, *Phys. Rev.*, **17**, 273 (1921), <https://doi.org/10.1103/PhysRev.17.273>
- <sup>40</sup> Z. Peršin, R. Zaplotnik and K. Stana Kleinschek, *Text. Res. J.*, **84**, 140 (2013), <https://doi.org/10.1177/0040517513485631>
- <sup>41</sup> O. P. Marg and H. Khas, "Absorption Spectroscopy", CSMRS, New Delhi, 2000
- <sup>42</sup> X. Liu, Y. Niu, K. C. Chen and S. Chen, *Mater. Sci. Eng. C*, **71**, 289 (2017), <https://doi.org/10.1016/j.msec.2016.10.019>
- <sup>43</sup> L. Fras Zemljic, O. Plohl, A. Vesel, T. Luxbacher and S. Potrč, *Int. J. Mol. Sci.*, **21**, 495 (2020), <https://doi.org/10.3390/ijms21020495>
- <sup>44</sup> A. N. B. Romainor, S. F. Chin, S. C. Pang and L. M. Bilung, *J. Nanomater.*, **41**, 1 (2014), <https://doi.org/10.1155/2014/710459>
- <sup>45</sup> M. M. Amrei, M. Davoudi, G. G. Chase and H. V. Tafreshi, *Sep. Purif. Technol.*, **180**, 107 (2017), <https://doi.org/10.1016/j.seppur.2017.02.049>
- <sup>46</sup> T. Luxbacher, "The Zeta Potential for Solid Surface Analysis", Anton Paar GmbH, 2014
- <sup>47</sup> T. Isogai, T. Saito and A. Isogai, *Biomacromolecules*, **11**, 1593 (2010), <https://doi.org/10.1021/bm1002575>
- <sup>48</sup> J. Praskalo, M. Kostic, A. Potthast, G. Popov, B. Pejic *et al.*, *Carbohydr. Polym.*, **77**, 791 (2009), <https://doi.org/10.1016/j.carbpol.2009.02.028>
- <sup>49</sup> T. Nikolic, M. Korica, J. Milanovic, A. Kramar, Z. Petronijevic *et al.*, *Cellulose*, **24**, 1863 (2017), <https://doi.org/10.1007/s10570-017-1221-1>
- <sup>50</sup> D. Marković, M. Korica, M. Kostić, Z. Radovanovic, Z. Šaponjić *et al.*, *Cellulose*, **25**, 829 (2018), <https://doi.org/10.1007/s10570-017-1566-5>
- <sup>51</sup> J. Milanovic, M. Kostic, P. Milanovic and P. Skundric, *Ind. Eng. Chem. Res.*, **51**, 9750 (2012), <https://doi.org/10.1021/ie300713x>
- <sup>52</sup> J. Milanovic, S. Schiehser, P. Milanovic, A. Potthast and M. Kostic, *Carbohydr. Polym.*, **98**, 444 (2013), <https://doi.org/10.1016/j.carbpol.2013.06.033>
- <sup>53</sup> Ā Gulcin, *Arch. Toxicol.*, **94**, 651 (2020), <https://doi.org/10.1007/s00204-020-02689-3>
- <sup>54</sup> K. W. Kim and R. L. Thomas, *Food Chem.*, **101**, 308 (2007), <https://doi.org/10.1016/j.foodchem.2006.01.038>
- <sup>55</sup> W. Xie, P. Xu and Q. Liu, *Bioorg. Med. Chem.*

*Lett.*, **11**, 1699 (2001), [https://doi.org/10.1016/S0960-894X\(01\)00285-2](https://doi.org/10.1016/S0960-894X(01)00285-2)

<sup>56</sup> M. Saljoughian, *US Pharm.*, **1**, 38 (2007), <https://www.uspharmacist.com/article/natural-powerful-antioxidants>

<sup>57</sup> E. F. Rostan, H. V. DeBuys, D. L. Madey and S. R. Pinnell, *Int. J. Dermatol.*, **41**, 606 (2002),

<https://doi.org/10.1046/j.1365-4362.2002.01567.x>

<sup>58</sup> E. Guibal, T. Vincent and R. Navarro, *J. Mater. Sci.*, **49**, 5505 (2014), <https://doi.org/10.1007/s10853-014-8301-5>

<sup>59</sup> J. B. Pristov, A. Mitrović and I. Spasojević, *Carbohydr. Res.*, **346**, 2255 (2011), <https://doi.org/10.1016/j.carres.2011.07.015>